# Coupling of pinned magnetic moments in an antiferromagnet to a ferromagnet and its role for exchange bias

OPEN ACCESS
IOP Publishing
Journal of Physics: Condensed Matter
J. Phys.: Condens. Matter **32** (2020) 075801 (8pp)
https://doi.org/10.1088/1361-648X/ab531a

# Coupling of pinned magnetic moments in an antiferromagnet to a ferromagnet and its role for exchange bias

**M Yaqoob Khan[1,2], Yasser A Shokr[1,3] and Wolfgang Kuch[1]**

[1] Institut für Experimentalphysik, Freie Universität Berlin, Arnimallee 14, 14195 Berlin, Germany
[2] Kohat University of Science and Technology, Kohat 26000, Khyber Pakhtunkhwa, Pakistan
[3] Faculty of Science, Department of Physics, Helwan University, 17119 Cairo, Egypt

E-mail: kuch@physik.fu-berlin.de

Received 12 August 2019, revised 2 October 2019
Accepted for publication 31 October 2019
Published 13 November 2019

**Abstract**

The interaction between uncompensated pinned magnetic moments within an antiferromagnetic (AFM) layer and an adjacent ferromagnetic (FM) layer responsible for the existence of exchange bias is explored in epitaxially grown trilayers of the form FM2/AFM/FM1 on $Cu_3Au(0\,0\,1)$ where FM1 is ~12 atomic monolayers (ML) Ni, FM2 is 21–25 ML Ni, and AFM is 27 ML or 50 ML $Ni_{\sim 25}Mn_{\sim 75}$. Field cooling for parallel or antiparallel alignment of the out-of-plane magnetizations of the two FM layers does not make a difference for the temperature-dependent coercivity ($H_C$), magnitude of exchange bias field ($H_{eb}$), AFM ordering temperature ($T_{AFM}$), and blocking temperature for exchange bias ($T_b$). We explain this by a model in which the uncompensated pinned magnetic moments distributed within the volume of the AFM layer interact with both of the FM layers, albeit with different strength. Parallel and antiparallel coupling between the magnetization of the pinned moments and the FM layers equally exists. This leads to the experimentally observed independence of $H_C$, $H_{eb}$, as well as of $T_{AFM}$ and $T_b$ on the magnetization direction of the FM layers during field cooling. These results provide new and detailed insight into revealing the subtle and complex nature of the exchange bias effect.

Keywords:exchange bias, antiferromagnet, magnetic interlayer coupling

Supplementary material for this article is available online

(Some figures may appear in colour only in the online journal)

## 1. Introduction

The pinning of a ferromagnetic (FM) layer by an adjacent antiferromagnetic (AFM) layer through the exchange bias (EB) effect is utilized in numerous applications of nanomagnetism, one of the most prominent being data storage, particularly on hard disk drives. They consist of small magnetic domains to represent data in the form of binary digits that are read out by a spin valve in the read head, utilizing the phenomena of giant or tunneling magnetoresistance [1–3]. The spin valve contains thin magnetic layers one of which is pinned by an adjacent AFM layer by the EB effect, creating a unidirectional anisotropy. An EB effect occurs between an FM and an AFM layer in contact and manifests itself as a shift of the hysteresis loop along the negative field axis after a field-cooling (FC) procedure [4–10].

The technological importance and interesting physics involved in EB has triggered massive research work to reveal its complex and subtle nature [4–23]. Initially, the EB effect was believed to be of interfacial nature [4, 5], which was backed by some models [6–9]. More recent findings showed that the effect is not purely an interfacial one but the AFM

bulk also plays a role [10–13], which is captured within the domain-state model [14–16]. It explains EB in terms of uncompensated pinned moments or pinning centers within the AFM layer. Recently, a review summarizing some important experimental evidence favors the notion that indeed the AFM bulk spin structure plays a key role in establishing the EB effect [10]. Notable is a study on a trilayer of the form FM/AFM/FM by Morales *et al*, which showed a significant difference in the exchange bias field between the parallel and antiparallel configurations of the two FM layers during field cooling. Therefore, the EB effect cannot be of purely interfacial origin and the bulk AFM contains uncompensated moments to pin the magnetizations of the adjacent FM layers in one direction [11]. Similar results have been obtained by Svalov *et al* [12]. However, since the samples involved in these experiments were polycrystalline and relatively thick [11, 12], the nature of the interaction of these uncompensated moments with the FM layer through the spin structure of the AFM layer could not be clearly explained.

Recently, we have shown that the behavior of the exchange bias effect of an FM/AFM bilayer upon placing a second FM layer at the other interface of the AFM layer can yield important information about the nature of the uncompensated pinned moments in the AFM layer [13]. In [13], we have epitaxially grown (Co/)Ni/$Ni_{25}Mn_{75}$/Ni(/Co) trilayers on a $Cu_3Au(0\,0\,1)$ substrate. The optional Co layers have been used to change the magnetization direction of the Ni films from perpendicular to the film plane into the film plane. The exchange bias at the bottom AFM/FM interface nearly does not change when the magnetization of the two FM layers in the trilayers (FM/AFM/FM) is perpendicular to each other but shrinks drastically once the magnetization direction of the two FMs is parallel [13]. We have interpreted this in a model of competing non-collinear pinning centers (PCs) throughout the entire thickness of the AFM $Ni_{25}Mn_{75}$ layer [13].

To understand the nature of the EB effect in every detail is very difficult; it varies from material to material and from system to system; even very sensitive techniques like x-ray magnetic circular or linear dichroism [24] and spin-polarized scanning tunneling microscopy [25] do not allow to establish an explicit link between the uncompensated spins in the AFM and the size of the EB effect. Replacing polycrystalline structures by single crystals has the advantage to better control the structural properties of the films, particularly at the FM/AFM interface [26]. We have chosen Ni/$Ni_{\sim 25}Mn_{\sim 75}$/Ni/$Cu_3Au(0\,0\,1)$ for our study. $Ni_xMn_{1-x}$ on $Cu_3Au(0\,0\,1)$ is a well-studied single-crystalline AFM system, the growth, structural and magnetic properties of which are known [13, 21, 22, 27, 28]. Whereas NiMn grows along the *a* axis on Cu(0 0 1) [29], on $Cu_3Au(0\,0\,1)$ it is oriented with the *c* axis along the film normal [27]. $Ni_{\sim 25}Mn_{\sim 75}$ exhibits layer-by-layer growth on $Cu_3Au(0\,0\,1)$ as well as on Ni/$Cu_3Au(0\,0\,1)$ [22, 27, 28]. $Ni_xMn_{100-x}$ as an AFM layer epitaxially grown on top of out-of-plane magnetized Ni/$Cu_3Au(0\,0\,1)$ leads to EB in a wide range of concentrations *x*, where a lower *x* results in a higher blocking temperature for EB as well as in higher EB fields [22, 28].

Trilayers of the form Ni/$Ni_{40}Mn_{60}$/Ni have been investigated on Cu(0 0 1), where the NiMn exhibits a spin-state transition, leading to a strong increase in interlayer coupling above a certain temperature [20]. On $Cu_3Au(0\,0\,1)$, on the other hand, the interlayer coupling is about one order of magnitude smaller for $Ni_{25}Mn_{75}$ of about 45 atomic monolayers (ML) thickness while sizeable EB is observed [21]. To the best of our knowledge, besides [13, 21], there is no previous work on EB in single-crystalline FM/AFM/FM trilayers.

Here, we study epitaxially grown trilayers ~25 ML Ni/*t* $Ni_{\sim 25}Mn_{\sim 75}$/~12 ML Ni on $Cu_3Au(0\,0\,1)$ using magneto-optical Kerr effect (MOKE) for exploring indirectly the physics behind the EB effect, where *t* stands for ~27 or ~50 ML thickness of $Ni_{\sim 25}Mn_{\sim 75}$. These thicknesses of the NiM layer have been chosen to be thick enough to show decent exchange bias [28] and a comparably weak interlayer exchange coupling. The two selected thicknesses for $Ni_{\sim 25}Mn_{\sim 75}$ do not make a qualitative difference in measuring the temperature-dependent magnetic properties. The thicknesses of the two FM Ni layers are selected to be different by about a factor of 2, in order to distinguish clearly their magnetization loops in the MOKE experiments. Setting the exchange bias for parallel or antiparallel magnetization of the Ni layers does not lead to any detectable difference in the absolute value of the exchange bias, in contrast to expectations for shared pinning centers for the two FM layers throughout the bulk of the AFM layer. We propose a simplified 1D model based on experimental findings in single-crystalline FM/AFM/FM layers. It consists of pinning centers across the volume of the antiferromagnet, which couple to the ferromagnets on each side of the antiferromagnet with a certain distribution of coupling strengths. This coupling is mediated by the antiferromagnetic exchange interaction inside the AFM material, leading to an equal amount of coupling paths of parallel and of antiparallel orientation between FM magnetization and the direction of the pinned magnetic moments. The model qualitatively describes the experimental results and is also consistent with our previous findings in (Co/)Ni/$Ni_{25}Mn_{75}$/Ni(/Co) trilayers on $Cu_3Au(0\,0\,1)$, where the EB is reduced in case of collinear easy axes of the two FM layers compared to noncollinear easy axes or the respective bilayer systems [13].

## 2. Experimental

All the experiments were performed under ultrahigh vacuum conditions with a base pressure of about $10^{-10}$ mbar. The single-crystalline $Cu_3Au(0\,0\,1)$ substrate was cleaned by sputtering with 1 keV $Ar^+$ ions and annealing at 800 K for 10 min. The AFM layer of $Ni_{\sim 25}Mn_{\sim 75}$ was grown by coevaporation of Ni and Mn from separate sources, in which high-purity (Ni: 99.99%, Mn: 99.95%) rods are bombarded by electrons while keeping the substrate at room temperature. Film thicknesses were calibrated by medium-energy electron diffraction and Auger electron spectroscopy. Approximately 12 ML Ni (FM1) was first deposited over the substrate, followed by a $Ni_{\sim 25}Mn_{\sim 75}$ layer of different thicknesses. The thickness of the top Ni layer (FM2) was 21–25 ML. Both Ni layers have an

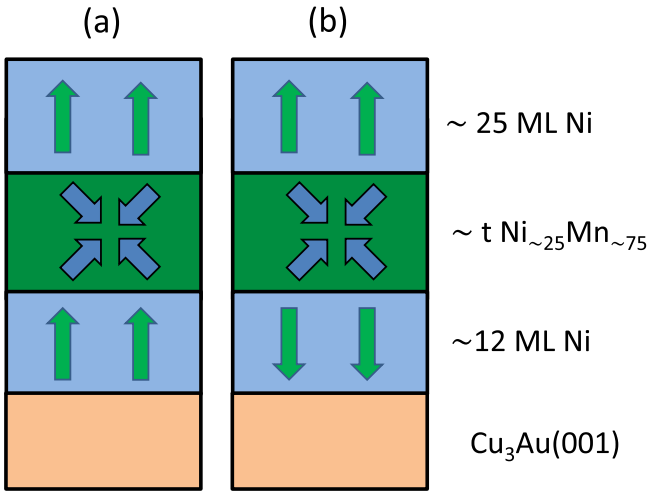


**Figure 1.** Schematic illustration of the two prepared samples of the FM2/AFM/FM1 trilayer system when the magnetizations of the two FM layers are (a) parallelly and (b) antiparallelly aligned. The approximate thicknesses of FM1, FM2, and AFM, as well as the approximate composition of the latter are shown, where *t* stands for ~27 or ~50 ML thickness of $Ni_{\sim 25}Mn_{\sim 75}$.

out-of-plane easy axis of magnetization. The accuracy of the thickness measurement is $\pm 1$ ML for $Ni_{\sim 25}Mn_{\sim 75}$ and sub-ML for Ni, the error in the Ni (Mn) concentration is less than $\pm 2$ percent points. Before each measurement series, the sample was first heated to above the ordering temperature $T_{AFM}$ of the AFM layer, which we know from our previous work [28], but below the Curie temperature of the FM layers, and then field-cooled (FC) to the minimum available temperature. Samples were FC either in the presence of a positive or a negative external magnetic field to get the parallel alignment of the two FM layers, or in such a way that one of the layers (FM1) is magnetized in the negative direction and the other (FM2) in the positive direction. The corresponding schematic drawing is shown in figure 1 for the trilayer to elaborate the situation. Magnetization loops are subsequently recorded using polar MOKE, while increasing the temperature from lower to higher values, starting at the temperature above which the available field of $\pm$ 200 mT allowed to reach magnetic saturation. Linearly polarized laser light of 1 mW power and 635 nm wavelength was used for the *in situ* polar MOKE measurements. For these measurements, the sample was placed in a glass tube sitting in between the two poles of an electromagnet. A straight line was subtracted from the resulting magnetization loops to account for the Faraday effect of the glass.

## 3. Results and discussion

Figure 2(a) shows the temperature-dependent hysteresis loops for 25 ML Ni/50 ML $Ni_{21}Mn_{79}$/12.9 ML Ni/$Cu_3Au$(0 0 1) when both FM layers are parallelly magnetized by a +10 mT external magnetic field during FC to give a negative EB shift. With the application of −10 mT for FC, temperature-dependent hysteresis loops are also measured which provided the very same EB shift along the positive direction (not shown). Figure 2(b) is for the loops when both the FM layers

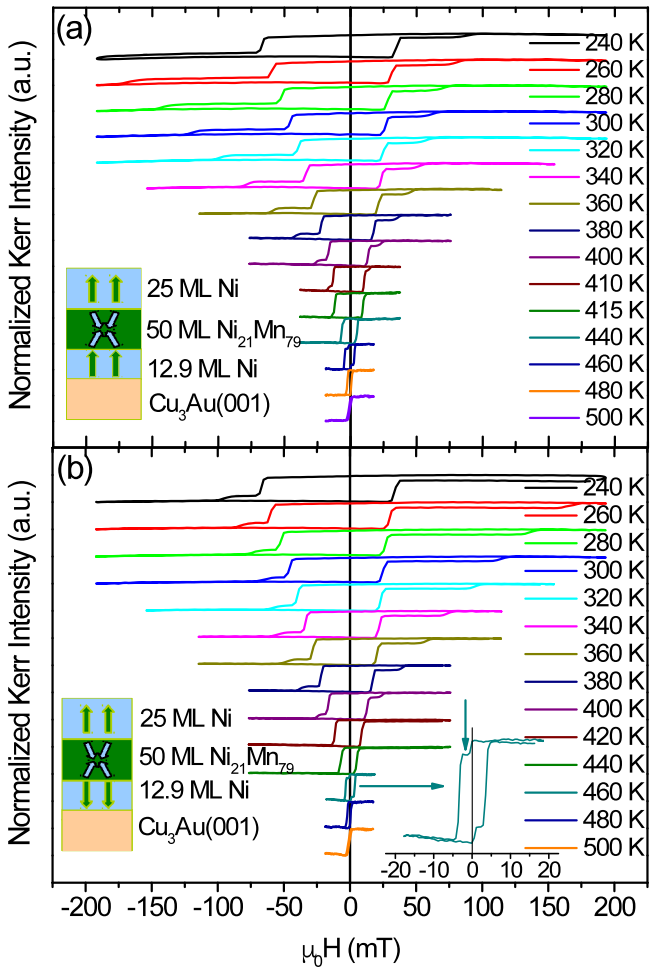


**Figure 2.** Normalized hysteresis loops for ~25 ML Ni/~50 ML $Ni_{21}Mn_{79}$/12.9 ML Ni/$Cu_3Au$(0 0 1) measured with polar MOKE at different temperatures. (a) Both interfaces give negative exchange bias when field-cooled with +10 mT from 510 K, and (b) opposite exchange bias shifts—the lower one positive, as it is field-cooled with −2 mT from 460 K (a zoomed-in loop is shown at this temperature with vertical down arrow representing the cooling field value), and the upper one a negative due to previous field-cooling with +10 mT.

are oppositely (antiparallelly) magnetized to provide one of the interfaces (top) with negative and the other one (bottom) with positive EB shift. To have both of the FM layers magnetized in opposite direction, the following procedure was applied during the FC process: After a field-cooling procedure with +10 mT field, the sample was again field-cooled from a temperature of 460 K with −2 mT. At this temperature FM2 has a smaller coercivity $H_C$ (0.9 mT) than FM1 (3.5 mT). Both the FM layers are now in antiparallel spin configuration, which by cooling through the blocking temperature $T_b$ gives opposite EB shift $H_{EB}$ at both interfaces; positive at the lower interface and negative at the upper one. For the parallel spin configuration of both the FM layers, the EB shift towards negative field can be observed from the double-step loop (both connected loops are shifted to the left side in figure 2(a)). For the antiparallel alignment of the FM layers' magnetization at both the interfaces, the negative (positive) shift due to EB at the upper (lower) interface is evident from the loops shown

in figure 2(b). Because of the smaller (almost half) thickness of FM1 compared to FM2, both EB and $H_C$ are larger for the lower interface than for the upper one, as expected. In both cases of parallel and antiparallel alignment of the two FM layers, $H_C(T)$ and $H_{eb}(T)$ decrease with increasing temperature. The two coercivities in a loop are well separated from each other below 420 K and above 440 K. At 420 K and at 440 K, the $H_C$ values for both of the loops coincide to give a single loop such that both of the FM layers are switching together in an externally applied magnetic field. Below (above) this temperature range (420 K–440 K), FM2 (FM1) switches before FM1 (FM2). At and above 480 K, there exists only a single loop for FM2, as FM1 becomes paramagnetic between 460 K–480 K.

Figures 3(a) and (b) respectively show the temperature-dependent $H_C$ and $H_{eb}$ data for the two trilayer samples: the first one ~25 ML Ni/~50 ML $Ni_{21}Mn_{79}$/12.9 ML Ni/$Cu_3Au$(0 0 1) and the second one 22 ML Ni/27 ML $Ni_{25}Mn_{75}$/11.9 ML Ni/$Cu_3Au$(0 0 1). Data are shown for the case of parallel alignment of the FM layers (black and red symbols) and for the case of antiparallel alignment (green and blue symbols) due to the procedure mentioned above. It is to be noted that one of the data sets (red symbols for 27 ML $Ni_{25}Mn_{75}$) has been already reported by us in [13]. The $H_C(T)$ ($H_{eb}(T)$) data overlap for the same interface in the cases of parallel and antiparallel magnetization alignment of the two FM layers in both samples (black and green for FM2/AFM, red and blue for AFM/FM1). The $H_C(T)$ and $H_{eb}(T)$ values for the lower interface (AFM/FM1) are about two times that of the upper interface (FM2/AFM), due to the thickness of FM1 being almost half of that of FM2 and the well-known inverse behavior of $H_{eb}$ with FM thickness. Very identical $H_C(T)$ and $H_{eb}(T)$ dependencies, as well as similar values of $T_{AFM} \approx 450$ K (≈420 K) and $T_b \approx 400$ K (≈340 K) for both interfaces are observed in all the samples. This is probably due to a very similar morphology/roughness at both interfaces of the samples. Very similar results (given as supplementary material (stacks.iop.org/JPhysCM/32/075801/mmedia)) are obtained for another trilayer 25 ML Ni/47 ML $Ni_{17}Mn_{83}$/12.9 ML Ni/$Cu_3Au$(0 0 1).

Was the EB effect a purely interfacial phenomenon, this result would not be surprising. The two interfaces would then be independent from each other and would have no effect on each other. However, as outlined in the introduction, this is not the case. In fact, EB is a bulk phenomenon. We have previously shown that trilayers of the form FM/AFM/FM with collinear magnetization directions of both FM layers exhibit always a much lower exchange bias field $H_{eb}$ at a fixed temperature and also show a significantly reduced blocking temperature $T_b$ for EB compared to bilayers with the same AFM layer and to trilayers with orthogonal easy axes (in-plane and out-of-plane) of the two FM layers [13]. In the latter, both $H_{eb}$ and $T_b$ are nearly identical to that of the corresponding bilayers. Such a behavior can be explained by assuming pinned magnetic moments inside the bulk of the AFM layer that coexist independently for orthogonal spin directions but have to be equally shared between both interfaces in the case of collinear

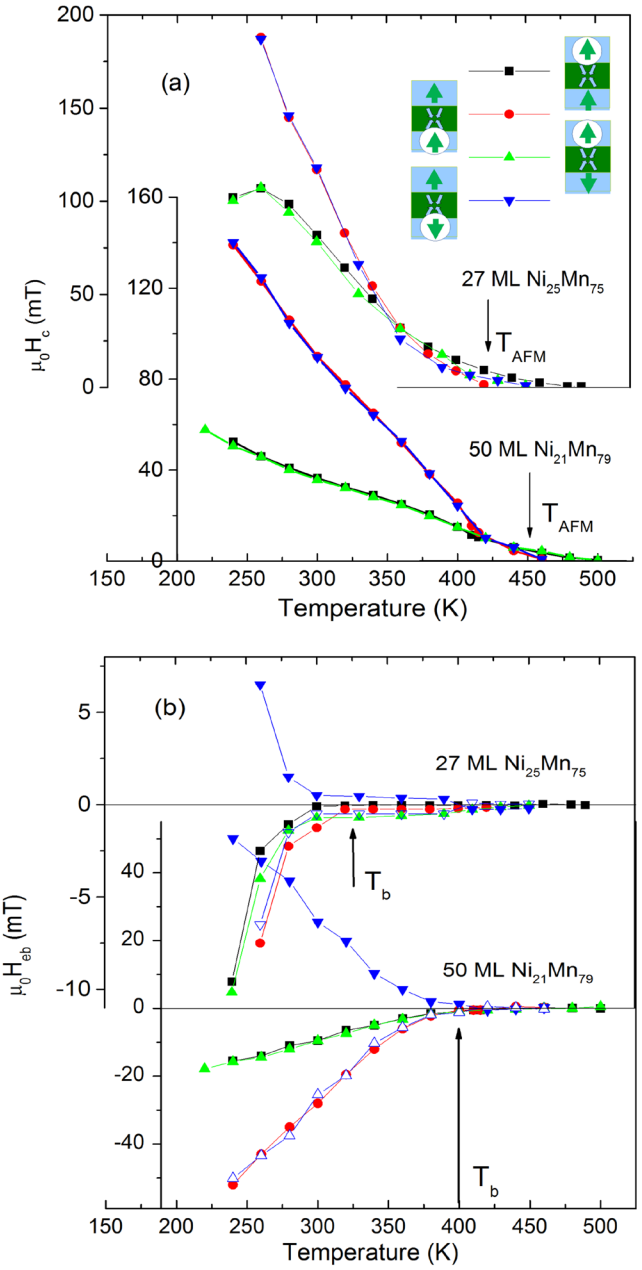


**Figure 3.** Temperature dependence of coercivity (a) and exchange-bias field (b) for ~25 ML Ni/~50 ML $Ni_{21}Mn_{79}$/12.9 ML Ni/$Cu_3Au$(0 0 1) and 22 ML Ni/27 ML $Ni_{25}Mn_{75}$/11.9 ML Ni/$Cu_3Au$(0 0 1), measured with polar MOKE. The different spin configurations of the FM layers at the upper and lower interface are symbolically shown in front of the corresponding legend. The antiferromagnetic ordering temperature $T_{AFM}$ and blocking temperature $T_b$ are indicated in both figures by arrows. Open blue symbols in (b) represent a mirror of the same-color filled symbols with positive EB.

spin directions [13]. Therefore, in the light of this explanation, the temperature-dependent $H_C$ and $H_{eb}$ as well as $T_{AFM}$ and $T_b$ are already reduced for the trilayers under study here as compared to the corresponding bilayers or to trilayers with orthogonal magnetization of the two FM layers. In the following, we present a model that explains both, the identical behavior for parallel and antiparallel collinear magnetization

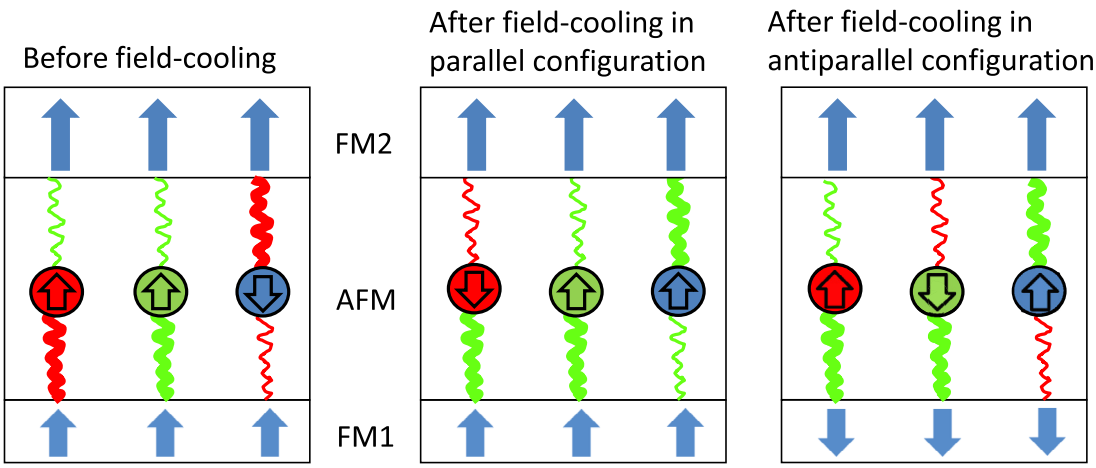


**Figure 4.** Sketch illustrating the proposed model by showing three examples of PCs in the AFM layer (colored circles with up/down arrows) between two collinearly magnetized ferromagnetic layers before and after field cooling as mentioned in the text. Before field cooling, the coupling of the PCs to both of the FM layers can be favorable (green curly lines) or unfavorable (red curly lines) depending on the detailed nature of the coupling path. The strength of the coupling is indicated by the thickness of the connecting curly lines. During field cooling, the direction of the PCs aligns according to the direction defined by the stronger of the two exchange paths. EB is enhanced by the favorably coupled PCs whereas it is reduced by the unfavorably coupled ones.

as well as the reduced EB compared to the case of different easy axes of the two FM layers.

It is nowadays commonly believed that EB is due to uncompensated pinned moments which arise due to a structural or chemical disorder that exists either at the surface/interface or within the volume of the AFM layer. Following the idea of the domain-state (DS) model [14, 15], we assume a random distribution of such PCs within the AFM layer. We do not need to specify the exact nature of these PCs. In the chemically disordered NiMn alloys, local concentration differences of Ni and Mn atoms, the latter with a tendency to antiferromagnetic nearest-neighbor exchange interaction, can lead to preferred positions of domain walls and can constitute the suggested pinning centers. Theoretical calculations for ordered bulk NiMn alloys have resulted in vanishing magnetic moments on the Ni sites due to the competing ferromagnetic Ni–Ni and antiferromagnetic Mn–Ni interactions [30]. In the disordered NiMn alloys the presence of local defects with small magnetic moments is thus feasible and could constitute the defects in the sense of the domain-state model of [14]. Once these pinned moments magnetically couple to the FM layer via interfacial spins, they become relevant for EB. During FC, the magnetization direction of the pinned moments will align in such a way that the coupling to the field-oriented FM magnetization is energetically favorable.

PCs with a magnetization component collinear to the FM layer magnetization couple to the FM layers. Coupling strength and sign are statistically distributed. We assume the coupling to be mainly due to direct exchange through the AFM spin structure. The coupling strength may be determined by the distance to the interface, but possibly also by other factors such as atomic-scale interface details, but it cannot be changed by field cooling. In the case of collinear magnetization of the two adjacent FM layers, PCs have to be commonly shared by both of the FM layers on either side. Before field-cooling, on average the same amount of PCs couple favorably and unfavorably to the FM layer, resulting in a vanishing EB effect. The favorable spin direction may be parallel or antiparallel to the FM layer magnetization, depending on the statistically distributed sign of the coupling. This is reasonable, since the sign of the coupling changes on the lengthscale of single-atomic distances for direct exchange coupling through an AFM spin structure. In a very simple picture, if the coupling path is one atom longer, it may reverse between parallel and antiparallel. We thus talk of ‘favorable’ and ‘unfavorable’ rather than of ‘parallel’ and ‘antiparallel’, since the individual coupling paths can favor either parallel or antiparallel alignment between the pinning center and the FM layer, depending on the atomistic details of the position of the pinning center with respect to the interfaces. ‘Unfavorable’ coupling of the pinning centers to the FM layers could mean a twist of the spins within the AFM layer between FM layer and pinning center, but could as well result from a higher level of frustration in the interface coupling with the FM layer or close to the actual pinning sites. In this model, we neglect coupling between such PCs, assuming that the average distance between two PCs is larger than the thickness of the AFM layer.

Figure 4 illustrates this situation. Three exemplarily chosen PCs are depicted in the middle of the AFM layer. Green and red lines connecting them to the two FM layers represent favorable and unfavorable coupling, where the line thickness indicates the coupling strength. Upon field cooling, the pinning centers adapt to the configuration of lowest energy, while the coupling remains fixed. This is sketched in figure 4 by the reversal of the spin direction of some of the PCs. During field cooling, a pinning center that was favorably but more weakly coupled to one layer and unfavorably but stronger to the other (like the red PC) will reverse, to result in an unfavorably weak coupling to the first layer and a favorably stronger one to the other. In this model, it is not possible for this particular pinning center to have favorable coupling to both layers since the nature of the coupling path does not change during field-cooling. PCs such as the red one in figure 4 thus explain the results of [13] and lead to a lower exchange bias in the case

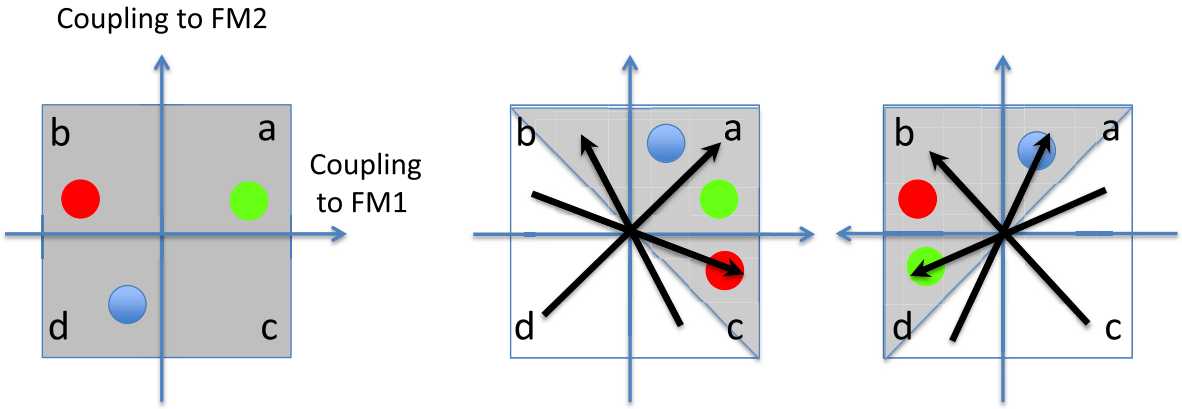


**Figure 5.** Schematic 2D graphs of the distribution of the coupling strength between the PCs and FM1 and FM2 along the horizontal and vertical axes of the graph, respectively. The grey-colored areas illustrate the distribution of different PCs within the AFM layer. The left graph shows the as-grown situation. The colored circles within the grey-colored areas represent the three examples for PCs already shown in figure 4, linking to the red, green, and blue PCs depicted there. (Left) Before field-cooling, on average there is an equal number of favorable (positive) and unfavorable couplings (negative) between the PCs and the FM layers resulting in no exchange bias. (Middle) Sample field-cooled in a parallel configuration. Half of the PCs have reversed their magnetization to minimize the total coupling energy to the two FM layers, indicated by the black arrows. The white regions are now depleted of PCs, which have moved to the grey-colored areas. Quadrant '(a)' contains PCs coupled favorably to both FM layers whereas grey-colored areas in quadrants '(b)' and '(c)' reduce the EB compared to independent, i.e. non-collinear configuration as discussed in [13]. (Right) Sample field-cooled in an antiparallel configuration. Similar to the middle sketch, but now favorable coupling to FM1 is on the left-hand side. Note that the grey-colored areas after field-cooling have the double density of PCs compared to before FC.

of collinear magnetizations of the FM layers in the FM/AFM/FM trilayers compared to bilayers. If the magnetization of one of the FM layers is reversed, however, this pinning center can orient during field cooling to establish favorable coupling to both FM layers in the antiparallel configuration (right-hand side).

The other two examples selected in the sketch of figure 4 are PCs that are unfavorably or favorably coupled to both sides as long as the two FM layers are magnetized in parallel, which means that they have to show unfavorable coupling to one of the FM layers in the case of antiparallel configuration. Since the coupling paths are statistically distributed, the EB after FC will be the same in both situations. This is not seen from figure 4, since it shows only three examples the average of which is not representative for all PCs, but can be illustrated by another type of sketch in figure 5: Here we show the distribution of coupling energies of pinned moments in the AFM layer to the two FM layers in a 2D graph. The coordinate system represents the coupling to FM1 (horizontal axis) and to FM2 (vertical axis). Zero is in the center. The colored circles represent the three examples from figure 4. For the as-grown trilayer, a situation as shown in the left sketch of figure 5 is present: For a parallel alignment of FM1 and FM2, positive values mean a favorable coupling between pinning centers and FM layer, while negative values mean unfavorable alignment (against the coupling energy). The grey-colored area illustrates the distribution of pinned moments, which is symmetric in the as-grown case, i.e. there are as many favorable as unfavorable coupling paths between FM layers and pinning centers. We do not need to assume any specific distribution function; the boundary of the grey-colored area does not need to be sharp. Important is that it is fourfold symmetric. On average, there is thus no EB.

The middle panel of figure 5 shows the situation after FC in a parallel configuration of FM1 and FM2. Pinned moments from quadrant (d), which were coupled in an unfavorable way to both FM layers, have now reversed their magnetization direction and couple favorably to both FM layers, i.e. have moved to quadrant (a). An example is the blue PC from figure 4, which is represented by a blue symbol in figure 5. Reversing the magnetization of pinned moments in the sketch means mirroring their position in the graph with respect to the origin. In quadrant (a) pinned moments are coupled favorably to both FM layers, contributing to EB for both layers. An example is the green PC from figure 4, again represented by a green symbol in figure 5. In quadrants (b) and (c), pinned moments couple favorably to one of the FM layers and unfavorably to the other. Their behavior during FC then depends on the relative strength of the couplings. The pinning centers for which the unfavorable coupling would be stronger than the favorable one reverse their magnetization during the field-cooling process, indicated by the black arrows in figure 5. Pinning centers are thus only left in the grey-colored areas of quadrants (b) and (c) in the middle sketch. The ones in the grey-colored area of quadrant (b) enhance the EB of layer FM2, but reduce the one of layer FM1, while the pinned moments in the grey-colored area of quadrant (c), like the red example from figure 4, enhance the EB of layer FM1 and reduce the one of layer FM2. The pinned moments in quadrants (b) and (c) are responsible for the reduction of the EB in case of collinear magnetization of FM1 and FM2 compared to perpendicular magnetization directions, as observed in [13]. The EB of layer

FM1 results from an integration of the horizontal component of all pinned moments in the sketch after field cooling, the EB of layer FM2 from an integration of the vertical component.

The situation after FC under antiparallel magnetization directions of FM1 and FM2 is depicted on the right-hand side of figure 5. Here we assume that compared to the middle sketch the magnetization direction of FM1 is opposite during FC. Now the pinning centers in quadrant (b) are coupled favorably to both FM layers, while the ones in quadrant (c) would be coupled unfavorably to both layers. The latter thus reverse their magnetization direction in the field-cooling process, which puts them also in quadrant (b). For the pinning centers in quadrants (a) and (d) now the same applies as discussed before in the parallel case for quadrants (b) and (c). Pinned moments in quadrant (a) are coupled favorably to FM2, but unfavorably to FM1. If the coupling to FM1 is stronger than the one to FM2, they reverse their magnetization direction during FC and thus move to quadrant (d), as indicated by arrows. The green PC from figure 4 is an example of that. In the same way, half of the pinning centers from quadrant (d) move to quadrant (a), like the example of the blue PC. Since the distribution of coupling paths is symmetric, the resulting EB for both layers is exactly the same as for the parallel situation shown in the middle sketch. Now the EB for layer FM1 results from the integration of the negative horizontal component of the pinning centers in the sketch.

Our model explains nicely the experimental findings of [13] and the ones presented here. In the case of perpendicular magnetization of the two FM layers, like in [13], only pinning centers with an oblique magnetization direction have to be shared by the two FM layers, while all predominantly out-of-plane pinning centers contribute to the EB of the out-of-plane FM layer, and all predominantly in-plane pinning centers contribute to the EB of the in-plane FM layer. When both layers are magnetized collinearly, one type of pinning centers does not play any role, while the other type has to be shared between the two FM layers, leading to the occurrence of unfavorable coupling, as described by our model, and thus a smaller EB, as observed experimentally [13]. A weaker overall unidirectional coupling after FC results also in a lower blocking temperature for EB, as also observed experimentally. Our model provides a qualitative picture for one of the essential ingredients for exchange bias, namely the connection between the PCs, which serve as a memory of the field cooling procedure and provide the symmetry breaking necessary for unidirectional anisotropy, and the ferromagnetic layer. From symmetry arguments, the resulting exchange bias properties of the two FM layers in a trilayer should not depend on whether the two FM layers are magnetized in parallel or antiparallel during the field cooling.

It does, however, not explain the results from polycrystalline samples of Morales *et al* for 50 nm Ni/200 nm $FeF_2$/50 nm Py [11] and those of Svalov *et al* for 30 nm FeNi/10 or 15 nm FeMn/10 nm FeNi [12], which are also in contrast to our experimental results obtained on the epitaxial trilayer systems. The authors of [11] do not offer a microscopic explanation of their result, but discuss it by antiferromagnetic domains extending from the two interfaces, creating maximum EB for the parallel case, while opposite AFM domains, leading to the formation of domain walls in the bulk of the AFM layer, are created in the antiparallel case [11]. The polycrystalline and relatively thick (200 nm) AFM layer may exhibit less clear paths for coupling. Since the direct coupling of the PCs with the FM layers on either side is less probable in these samples, they may also exhibit chains of PCs that are coupled collectively to the FM layers, the coupling between PCs may be of the same magnitude as the coupling to the FM layers, or one sign of the coupling between the PCs and the FM layers is preferred over the other. Another possibility is a different magnetic structure within the bulk of the AFM ($FeF_2$) after field cooling in the two configurations that could result from some remaining AFM magnetic order still being present above the Néel temperature, for example from proximity effects between AFM and FM materials [31]. A different, more tilted shape of the hysteresis loops of the reported system on changing the configuration of the two FM layers from parallel to antiparallel has indeed been reported [11]. This is not the case in our study, as very similar rectangularly-shaped double coercivity loops can be seen for both configurations.

## 4. Conclusion

In conclusion, we can interpret our results by considering that in the single-crystalline system pinned magnetic moments are distributed within the entire volume of the AFM layer, both with in-plane and out-of-plane directions. For two trilayers with 27 ML and 50 ML $Ni_{\sim 25}Mn_{\sim 75}$ as an AFM layer sandwiched between two FM Ni layers magnetized in out-of-plane direction with thicknesses different by a factor of two, $H_C(T)$, the magnitude of $H_{eb}(T)$, as well as the values for $T_{AFM}$ and that for $T_b$ are found to be identical for the respective interfaces in each sample, no matter whether the system is field-cooled such that both the FM layers magnetizations are parallel or antiparallel to each other. The model we propose clearly explains all the results of this work as well as of our own previously obtained results for single crystalline samples with collinear and orthogonal easy axes of the two FM layers. In this model, we assume that the PCs responsible for EB are scattered randomly within the volume of the AFM layer and are coupled through exchange interaction to the FM layers on both sides. The coupling of the PCs can be stronger to one of the two FM layers but is not affected by field-cooling. The sign of the coupling can be parallel or antiparallel, depending on the detailed exchange path. The setting of the pinned moments during field cooling is then determined by the orientation of the FM layer to which the PC is more strongly coupled. On average, there will thus be as many moments coupled with the same sign (favorably) to both FM layers, as moments coupled with opposite sign (unfavorably). If all this is statistically averaged, the net pinning (the exchange bias) should not depend anymore on the actual orientation of magnetization, as we see it. These results clearly demonstrate that in epitaxially grown samples the AFM bulk spin structure plays a vital and distinct role in the establishment of EB.

## Acknowledgments

MYK is grateful for financial support during his stay in Berlin by the Higher Education Commission (HEC) of Pakistan through Kohat University of Science & Technology (KUST), Kohat, Pakistan, Freie Universität Berlin, and DAAD (Deutscher Akademischer Austauschdienst) (German Academic Exchange Service) through Grants No. 57068383 and 57243485. We thank T Shinwari for fruitful discussions.

## ORCID iDs

Wolfgang Kuch https://orcid.org/0000-0002-5764-4574

## References

[1] Wang Y, Song C, Wang G, Miao J, Zeng F and Pan F 2014 *Adv. Funct. Mater.* **24** 6806
[2] Baltz V, Manchon A, Tsoi M, Moriyama T, Ono T and Tserkovnyak Y 2018 *Rev. Mod. Phys.* **90** 015005
[3] Chappert C, Fert A and Van Dau F N 2007 *Nat. Mater.* **6** 813
[4] Meiklejohn W H and Bean C P 1956 *Phys. Rev.* **102** 1413
[5] Meiklejohn W H and Bean C P 1957 *Phys. Rev.* **105** 904
[6] Malozemoff A P 1987 *Phys. Rev.* B **35** 3679
[7] Malozemoff A P 1988 *Phys. Rev.* B **37** 7673
[8] Mauri D, Siegmann H C, Bagus P S and Kay E 1987 *J. Appl. Phys.* **62** 3047
[9] Koon N C 1997 *Phys. Rev. Lett.* **78** 4865
[10] Schuller I K, Morales R, Batlle X, Nowak U and Güntherodt G 2016 *J. Magn. Magn. Mater.* **416** 2
[11] Morales R, Li Z-P, Olamit J, Liu K, Alameda J M and Schuller I K 2009 *Phys. Rev. Lett.* **102** 097201
[12] Svalov A V, Kurlyandskaya G V, Lepalovskij V N, Savin P A and Vas'kovskiy V O 2015 *Superlattices Microstruct.* **83** 216
[13] Khan M Y, Wu C-B and Kuch W 2014 *Phys. Rev.* B **89** 094427
[14] Nowak U, Usadel K D, Keller J, Miltenyi P, Beschoten B and Güntherodt G 2002 *Phys. Rev.* B **66** 014430
[15] Keller J, Miltényi P, Beschoten B, Güntherodt G, Nowak U and Usadel K D 2002 *Phys. Rev.* B **66** 014431
[16] Miltényi P, Gierlings M, Keller J, Beschoten B, Güntherodt G, Nowak U and Usadel K D 2000 *Phys. Rev. Lett.* **84** 4224
[17] Ohldag H, Regan T J, Stöhr J, Scholl A, Nolting F, Lüning J, Stamm C, Anders S and White R L 2001 *Phys. Rev. Lett.* **87** 7201
[18] Ohldag H, Scholl A, Nolting F, Arenholz E, Maat S, Young A T, Carey M and Stöhr J 2003 *Phys. Rev. Lett.* **91** 17203
[19] Lederman D, Ramírez R and Kiwi M 2004 *Phys. Rev.* B **70** 184422
[20] Hagelschuer T, Shokr Y A and Kuch W 2016 *Phys. Rev.* B **93** 054428
[21] Shokr Y A, Erkovan M, Wu C-B, Zhang B, Sandig O and Kuch W 2015 *J. Appl. Phys.* **117** 175302
[22] Khan M Y, Wu C-B, Erkovan M and Kuch W 2013 *J. Appl. Phys.* **113** 023913
[23] Nogués J and Schuller I K 1999 *J. Magn. Magn. Mater.* **192** 203
[24] Nolting F *et al* 2000 *Nature* **405** 767
[25] Bode M, Vedmedenko E Y, von Bergmann K, Kubetzka A, Ferriani P, Heinze S and Wiesendanger R 2006 *Nat. Mater.* **5** 477
[26] Kuch W, Chelaru L I, Offi F, Wang J, Kotsugi M and Kirschner J 2006 *Nat. Mater.* **5** 128
[27] Macedo W A A, Gastelois P L, Martins M D, Kuch W, Miguel J and Khan M Y 2010 *Phys. Rev.* B **82** 134423
[28] Khan M Y, Wu C-B, Kreft S K and Kuch W 2013 *J. Phys.: Condens. Matter* **25** 386005
[29] Tieg C, Kuch W, Wang S G and Kirschner J 2006 *Phys. Rev.* B **74** 094420
[30] Spišák D and Hafner J 1999 *J. Phys.: Condens. Matter* **11** 6359
[31] Lenz K, Zander S and Kuch W 2007 *Phys. Rev. Lett.* **98** 237201